Exploration of suitable injector configuration for Dual-Mode Dual-Fuel Engine with Diesel and OMEx as High Reactivity Fuels

Antonio García, Javier Monsalve-Serrano*, Enrique José Sanchís and Álvaro Fogué-Robles

CMT - Motores Térmicos, Universitat Politècnica de València, Camino de Vera s/n, 46022 Valencia, Spain

Fuel 280 (2020) 118670
https://doi.org/10.1016/j.fuel.2020.118670

Corresponding author (*):
Dr. Javier Monsalve-Serrano (jamonse1@mot.upv.es)
Phone: +34 963876559
Fax: +34 963876559

Abstract

Dual-mode dual-fuel (DMDF) combustion stands over other low temperature combustion strategies as it is able to operate over the entire engine map by transitioning between reactivity controlled compression ignition and diffusive combustion depending on the engine load. In combination with non-sooting e-fuels, it is able to achieve low NOx and soot levels even at high loads. Oxygenated fuels like poly-oxymethylene dimethyl ethers (OMEx) have been already proved to present an outstanding NOx-Soot trade-off improvement when used in combination with a DMDF combustion strategy. One drawback of OMEx is that, despite having a high reactivity, it has a low lower heating value, which requires considerably longer injection events compared to other traditional fuels in order to achieve the same engine power output. The long injections limit the flexibility of the injection strategy and result in extremely long combustion durations. A possible solution to this problem resides in moving towards injectors with higher flow rate capacities, but this may compromise the mixing and combustion processes. This work aims to shed some light on the implications of changing the engine hardware to overcome this limitation by testing a DMDF multi-cylinder engine using gasoline as the

low-reactivity fuel and diesel or OMEx as the high reactivity fuels with injectors of different flow capacity. The results show that a concise analysis of the involved phenomenology of the combustion process allows to find out the trade-off between the engine-out emissions and the mixing capacity of the injection system while the engine performance is not significantly affected.

Keywords

Dual-fuel; high-flow injector; emissions; Diesel; OMEx

1. Introduction

The current scenario for transport vehicles presents a wide variety of options for the main power source of the engines of the future. The decision for the manufacturers is very complex and they have to consider conditionings like the geographic zone, the vehicle platform or the target market [1]. Despite the increasing feasibility of electric vehicles, internal combustion engines (ICE) continue to be the main power source for the transport sector in the near future [2]. To ensure a more responsible and development of the fuels and powertrains of the future, some guidelines have already been decided [3]. The general purpose of these norms is to ensure that the future engines will be more efficient and clean while the fuels will tend to be more related to renewable sources and will present better combustion performance [4][5]. On the road map towards these long-term objectives, some more specific targets are implanted by the emissions regulations in the short term. Specifically, the projected normative for 2025 aims to reduce the CO_2 emissions for heavy-duty vehicles by 15%, which are mainly used for road transportation and represent a considerable percentage of the total CO_2 emissions despite the reduced number of vehicles [6][7]. In order to fulfil these requirements in the near-future, ICEs are expected to suffer an improvement in their

efficiency in order to maintain their actual power levels but consuming less fuel, and therefore emitting less contaminants [8].

Several developments were achieved during the last years in the powertrain field. An interesting example is the addition of electric devices to the vehicles, which provides a new degree of freedom in the powertrain design, allowing to recuperate energy from braking and from the exhaust gases [9], making this energy available during the vehicle operation to start-stop actions and to heat-up the aftertreatment devices to shorten the light-off period [10]. Despite of this, the ICE is still the kernel of the powertrain where most of the optimization effort is dedicated [11]. Some successful developments where presented along the years like direct injection engines fueled with gasoline [12], better downsizing strategies, injection systems with higher flow capacity for diesel engines, improvements in the after-treatment systems, further knowledge on the sources of energy losses in the combustion process and development of materials that allow to increase the stress tolerances [13][14]. Despite all these advances, it results to be very challenging to improve the efficiency of the diesel engine without having a trade-off with engine-out emissions [15]. New combustion concepts are being investigated to overcome this limitation, among which the low temperature combustion (LTC) results to be one of the most promising concepts. The most popular LTC concept is the homogeneous charge compression ignition (HCCI) that is primarily based on a very lean premixed combustion that allows a great potential to emit very low NOx and soot production with high efficiencies [16]. The main drawback of the highly premixed combustion is that it is restricted to a narrow operating region of the map due to limitations of mechanical stresses if the load is high [17] and misfire or incomplete

combustion with high production of CO and unburned hydrocarbons (HC) if the load is too low [18].

An equally promising LTC concept so called reactivity controlled compression ignition (RCCI) was developed considering more detailed knowledge on the reaction kinetics of fuels during combustion [19][20]. By using two fuels of different reactivity and producing a stratified charge in the cylinder, an in-cylinder reactivity stratification is forced as a consequence of the stratification of the fuel equivalence ratio and octane number [21][22]. This allows to widen the operational range of the HCCI while having low emissions levels, but it still is limited to medium load conditions [23][24]. An expansion of the RCCI concept was developed by Benajes et al. [25] which was called dual-mode dual-fuel (DMDF) combustion. This concept moves from partially premixed RCCI combustion at low loads to highly premixed RCCI combustion at medium loads and finally to a diffusive dual-fuel combustion at higher loads. This strategy allows to expand the dual-fuel combustion to cover the whole engine map keeping operability at high EGR (exhaust recirculated gases) rates that allow low NOx production, but with the drawback of being prone to soot production at higher loads due to the more diffusive combustion. This issue can be overcome by means of a hardware modification and/or a fuel modification. In this study, both alternatives will be explored.

Recent developments in the use and formation of alternative and synthetic fuels have found some potential fuels able to contribute to global CO_2 reduction during their life cycle while having good combustion performance. Thanks to the synthetic formulation of the compound, it is possible to obtain unadulterated fuels with no content of Sulphur or poly aromatic hydrocarbons that promote the formation of certain contaminants like

Sulphur oxides and soot, respectively [26]. Among these synthetic compounds, also known as electrolytic fuels or e-fuels, several options are being evaluated currently with good improvements with respect to the traditional fuel compositions. The majority of them are fuels focused on soot and NOx reduction with a low-carbon composition and an oxygenated or hydrogenated formulation to enhance the oxidation of soot and low lower heating values (LHV) to have a LTC that contributes to reduce the NOx formation [27].

Some of the most promising e-fuels are the hydrogenated vegetable oil (HVO), dimethyl ether (DME) or poly-oxymethylene dimethyl ethers (POMDME or OMEx) [28][29]. This last e-fuel is specially capable of soot and NOx reduction as reported in the existent investigations [30] with a formulation of high oxygen and low carbon composition, and it is possible to synthesize it using CO_2 capture from the atmosphere and some conversion steps [31][32].

Investigations addressing the use of these fuels in advanced combustion concepts like DMDF are still scarce, but clear consequences of the effect of the lower LHV have been reported in the existing literature [35][36]. Some applications of these chemicals involve using them as additives to other more energetic fuels like diesel to avoid high volumetric fuel consumption [33]. To fully exploit the advantages of these e-fuels they have to be used as a pure fuel instead of an additive, but then the high volumetric fuel consumption presents certain limitations on the operation of the engine mainly related to the long injection time needed to introduce sufficient energy content to achieve power requirements [37]. From the point of view of combustion control, the need of long injections when using pure e-fuels difficult the combustion phasing tuning and can affect

126 the emissions formation. When injection is too long and combustion ends too late, the
127 exhaust temperature can be excessively high for the turbine operational limits.
128 Additionally, the energy utilization during the expansion stroke can be detrimental and
129 diminish the output power or enhance HC and CO formation from the low temperature
130 combustion at the end of the expansion stroke [38]. This could be overcome with earlier
131 injections that promote a more premixed combustion mode, but the high reactivity of
132 e-fuels like OMEx produce strong heat releases with high in-cylidner pressures that can
133 damage the engine integrity due to large pressure gradients.

134 The aim of this work is to explore the possibility of using injectors with higher flow
135 capacity in order to reduce the injection time in a DMDF engine to overcome the
136 previously exposed limitations. For this investigation, the low reactivity fuel (LRF) will
137 always be gasoline and the high reactivity fuel (HRF) will be pure OMEx or pure diesel in
138 order to compare two different HRF compositions with different levels of LHV. Both will
139 be tested with two different set of injectors which have different flow rate capacities.
140 This concept come with uncertainties on the final behaviour of the combustion process
141 as with a higher flow rate, higher concentrations of fuel will be formed, and the mixing
142 capacity of the spray can be compromised depending on the fuel properties.

143 ## 2. Materials and methods
144 ### 2.1. Engine characteristics
145 The experimental evaluation of the different hardware and fuels has been carried out
146 using an 8L engine with 6 cylinders. The engine has been modified to permit the DMDF
147 operation: compression ratio has been reduced from the original 17.5:1 to 12.75:1 to
148 reduce mechanical stresses at high load conditions, the piston geometry has been
149 optimized in previous studies for the current combustion mode [22], and auxiliary

systems have been added, like the addition injection system or the low-pressure EGR circuit for greater flexibility on the control of the combustion process and engine-out emissions. The main features of the engine are summarized in Table 1.

Table 1. Engine characteristics.

Engine Type	4 stroke, 4 valves, direct injection
Number of cylinders [-]	6
Displaced volume [cm^3]	7700
Stroke [mm]	135
Bore [mm]	110
Piston bowl geometry [-]	Bathtub
Compression ratio [-]	12.75:1
Rated power [kW]	235 @ 2100 rpm
Rated torque [Nm]	1200 @ 1050-1600 rpm

2.2. Test cell description

In order to control and register the operation of the engine, a set of additional systems are included in the test facility and connected to the engine according to the diagram presented in Figure 1. For the engine control, an in-house interface developed in LabView interacts with all the hardware through a NI PXIe 1071 board and is responsible for the control of the engine load through both injection systems (the por-fuel injection (PFI) and direct injection (DI)), EGR valves, back pressure valve and VGT positioning. For the referencing of the injection timing and its duration, the crank shaft angular position is registered through and encoder. Separately, the engine speed is dictated by an active dynamometer from AVL that is controlled through the manufacturer user interface ALV PUMA open.

The same LabView platform is connected to all the measuring devices that include: several temperature and pressure sensors located at relevant locations of the flow circuits (including intake and exhaust manifolds), the six in-cylinder pressure signals with

a resolution of 0.2 crank angle degree (CAD), two balances to obtain fuel consumption of the HRF and LRF, and air flow meter at the intake, a five-gas Horiba MEXA-7100 DEGR analyser [39] and an AVL smoke meter for emissions measurement [40]. The models and accuracy of the main measuring devices is included in Table 2.

Both the LabView interface and the AVL PUMA open offer online readings of all the variables. Additionally, a real time processing routing is implemented in LabView that allows for instantaneous visualization of thermodynamic variables like the apparent heat release. The recording of the signals is divided into instantaneous variables and average variables, that the PXI and AVL PUMA perform respectively. Finally, the data collected from each test is post-processed with the software developed at CMT, called CALMEC, that allows for a more specific analysis of the in-cylinder thermodynamic evolution [41].

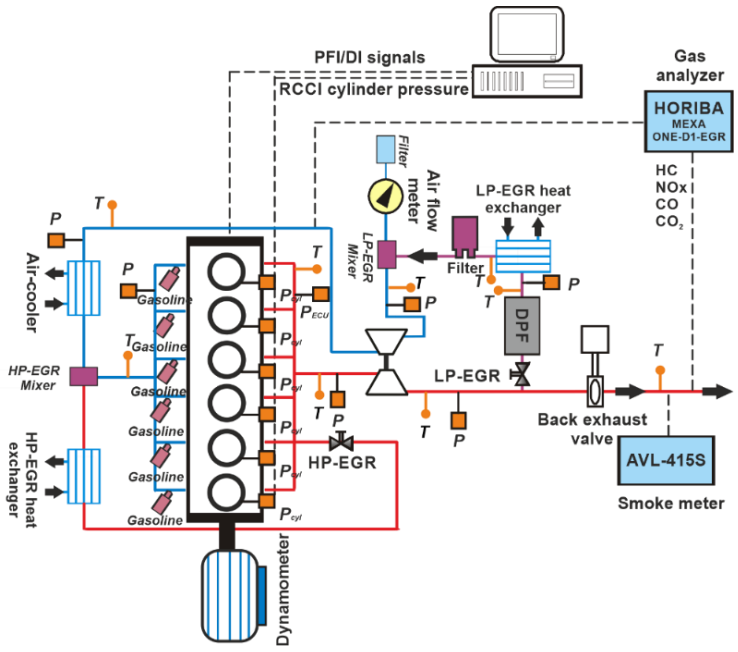

Figure 1. Experimental facility scheme.

Table 2. Accuracy of the instrumentation used in this work.

Variable measured	Device	Manufacturer / model	Accuracy
In-cylinder pressure	Piezoelectric transducer	Kistler / 6125C	±1.25 bar
Intake/exhaust pressure	Piezoresistive transducers	Kistler / 4045A	±25 mbar
Temperature in settling chambers and manifolds	Thermocouple	TC direct / type K	±2.5 °C
Crank angle, engine speed	Encoder	AVL / 364	±0.02 CAD
NOx, CO, HC, O_2, CO_2	Gas analyzer	HORIBA / MEXA 7100 DEGR	4%
FSN	Smoke meter	AVL / 415	±0.025 FSN
Gasoline/diesel fuel mass flow	Fuel balances	AVL / 733S	±0.2%
Air mass flow	Air flow meter	Elster / RVG G100	±0.1%

2.3. Fuels and injection systems characteristics

As already mentioned, several fuels are used in this investigation. For the LRF, commercial gasoline is used in every case. As the HRF, two different fuels are used: commercial diesel and an OME mixture 3-5 (OME3 and OME5 are the main components of the mixture), referred in this document as OMEx. The main physicochemical properties of these fuels have been certified by the supplier and are summarized in Table 3.

Table 3. Physical and chemical properties of gasoline and the different high reactivity fuels evaluated.

	EN 228 gasoline	EN 590 diesel	OMEx
Density [kg/m^3] (T= 15 °C)	720	842	1067
Viscosity [mm^2/s] (T= 40 °C)	0.545	2.929	1.18
Cetane number [-]	-	55.7	72.9
Carbon content [% m/m]	-	86.2	43.6
Hydrogen content [% m/m]	-	13.8	8.82
Oxygen content [% m/m]	-	0	47.1
RON [-]	95.6	-	-
MON [-]	85.7	-	-
Lower heating value [MJ/kg]	42.4	42.44	19.04
Vapor pressure [hPa] (T=40 °C)	450-650	<10	32

In this dual-fuel engine, the LRF is injected in the intake port with six port-fuel injectors (PFI) located at the intake manifold forming an initial almost-homogeneous charge, and the HRF is injected during the compression stroke with a direct injection (DI). The

200 stratification of the charge is controlled with the amount of HRF injected and the SOI at
201 which the injection is performed. In this work, two different sets of injectors are
202 evaluated for the direct injection of the HRF, each of them with different nominal flow
203 rate. The injector with the higher flow capacity will be referred as the high-flow injector
204 (HFI) and the one with the lower nominal flow rate will be referred as the low-flow
205 injector (LFI). The different characteristics of the injectors used in the experiments can
206 be consulted in Table 4. An additional variable of the injection system is the rail pressure.
207 With increasing load, the amount of fuel injected through the DI increases, and in order
208 to maintain the injection times under reasonable values, the rail pressure has to be
209 increased. In these tests, the injection pressure ranges from 600 to 2000 bar, and it is
210 always kept at the minimum value possible to reduce the power losses from auxiliary
211 devices like the high-pressure pump.

212 Table 4. Characteristics of the direct and port fuel injectors.

Direct injector			Port fuel injector	
	HFI	LFI		
Actuation Type [-]	Solenoid	Solenoid	Injector Style [-]	Saturated
Steady flow rate @ 100 bar [cm^3/min]	2200	1300	Steady flow rate @ 3 bar [cm^3/min]	980
Included spray angle [°]	140	150	Included Spray Angle [°]	30
Number of holes [-]	6	7	Injection Strategy [-]	single
Hole diameter [μm]	244	177	Start of Injection [CAD ATDC]	340
Maximum injection pressure [bar]	2500	2500	Maximum injection pressure [bar]	5.5

213

214 **2.4. Testing methodology**

215 Eight engine operating conditions were chosen as the most representative conditions of
216 a real driving cycle and are meant to be adequate to evaluate the impact of the different
217 injector typologies used for the DI. For the HRF, diesel will be tested to establish the
218 reference performance for each injector and OMEx will be then evaluated as the low-
219 LHV e-fuel.

The eight conditions tested are represented in Figure 2. As it can be seen, they cover different zones of the engine calibration map: conditions 1 to 4 are representative of partially premixed combustion (10% and 25% of engine load), condition 5 is a highly premixed combustion (50% of engine load) and conditions 6 to 8 represent a predominant diffusive combustion (80% to 100% engine load). By having operating points covering critical regions of the map, different effects like soot production at high loads and strong premixed combustions at lower loads can be evaluated, producing and overall analysis of the engine performance, making more evident the effect of the injector typology with each fuel.

The settings used for each case are based on the original calibration of the diesel-gasoline DMDF [34] and have been adapted to ensure comparable and operable conditions for each point and the different fuels and hardware. All the presented results are average values of a population of measurements with a coefficient of variation (COV) of the indicated mean effective pressure (IMEP) lower than 5% to ensure a stable operation and measurement that is representative of the operating condition. Each measurement of composed by roughly 100 consecutive cycles that are post-processed independently and then averaged using CALMEC.

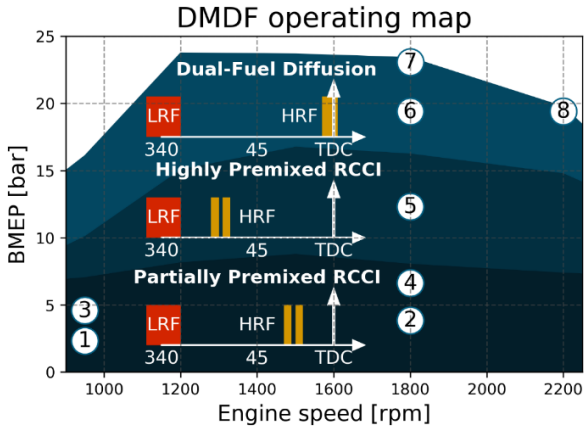

Figure 2. Evaluated operating conditions and the injection strategy at each zone of the map.

2.5. Spray model

The change injector characteristics and fuel properties affect the spray morphology and the fuel distribution inside the cylinder. For a more fundamental analysis of the changes in autoignition delay, the changes in the spray are evaluated using a one-dimensional spray model developed at CMT Motores Térmicos called DICOM [44]. This in-house model is designed to evaluate the spray temporal evolution under transient thermodynamic conditions to be able to evaluate in-cylinder fuel injections [45].

The fuel spray is assumed to develop as a fully developed turbulent flow with no additional directional flow nor obstacle in an infinite volume of air and EGR (composed of CO_2 and H_2O). This implies that no swirl effect or wall impingement can be considered, and the spray profile will be symmetric. The conservation equations for mass, species and momentum are solved for the central line using the discretization strategy depicted in Figure 3. Once that the velocity and thermodynamic properties are solved for the central line, it is possible to extend the hypothesis of the fully turbulent flow to apply self-similar radial profiles scaled with the diffusive properties of the fuel as expressed in Equation (1), where u is the axial velocity and f is the equivalence ratio. In this case a Gaussian profile is assumed. With this it is possible to obtain the mass fraction of fuel under discrete levels of equivalence ratio as will be shown in the results.

$$\frac{u(x,r)}{u_{cl}(x)} = \left(\frac{f(x,r)}{f_{cl}(x)}\right)^{1/Sc} = e^{-k\left(\frac{r}{x}\right)^2} \quad (1)$$

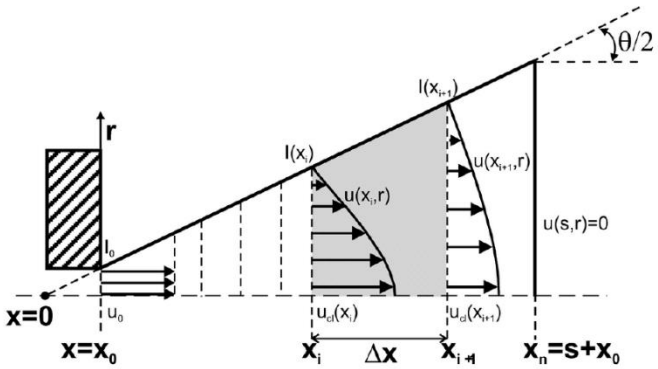

Figure 3. Spray model sketch.

The boundary conditions for the spray model that are needed as inputs are the ones characteristic to each operation, namely: the fuel composition (that allows for fuel mixtures), the thermodynamic conditions of the ambient gas that in this case will be pressure P(bar) and density ρ(kg/m^3) of the in-cylinder trapped mass, and the fuel mass flow rate $\dot{m}_{fuel}$(kg/s) that is used to compute the velocity u_0(m/s) and momentum I_0(kg·m/s) at the fuel input. The additional parameter related to the radial profile is the spray cone angle θ(deg), with which the parameter k from Equation (1) is defined. To define this parameter, it is possible to use additional semi-empirical correlations or impose a value. In this case the value of 22.5 (deg) was used as a representative value of diesel sprays [45].

2.6. Vehicle model

The final evaluation of the performance of each injector is carried out using the software GT-Power from Gamma Technologies® [48]. This software permits the modular design of a complete vehicle under imposed driving conditions based on zero-dimensional and one-dimensional models. The engine model uses the experimental results as an input to determine the engine effective power and total emissions of the complete driving simulation, and as it can be appreciated in Figure 4, a vehicle with specifications in accordance with the engine application was implemented considering factors like rolling

friction of components, road friction, aerodynamic resistance of the vehicle and the inertia of components like the axles or the transmission for the model to predict the instantaneous engine operating point [54].

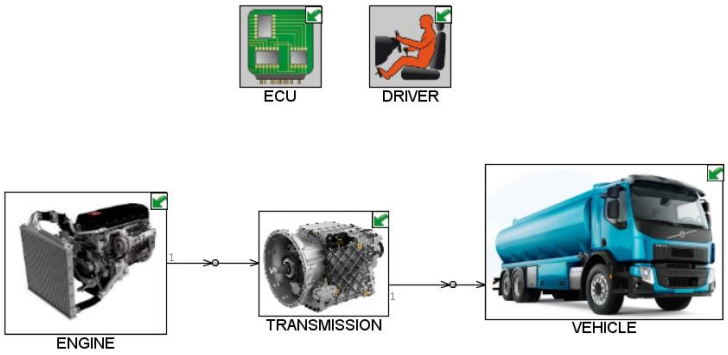

Figure 4. Main components of the vehicle simulation in GT-Power.

In compliance with the actual normative for homologation of transport heavy duty vehicles, as a general and representative case the World Harmonized Vehicle Cycle (WHVC) [49] is defined as the vehicle routine in the simulation with a payload of 50% of the maximum capacity of the vehicle [46]. In Table 5 are summarized the most relevant parameters used for the simulation, where the vehicle data is representative of a Volvo FE 350 truck with a gearbox of 12 gears and a shifting strategy designed to obtain the best performance of the engine [55].

Table 5. Main parameters of the vehicle model.

Engine displacement volume [cm^3]	7700
Engine control	Map based on experimental results [34]
Vehicle mass [kg]	7035
Cargo mass [kg]	8982.5
Frontal area [m^2]	6.89
Tires size [mm/%/inch]	295/80/22.5
Number of axles	3
Number of wheels	10
Vehicle wheelbase [m]	5
Final Drive Ratio [-]	3.08
Gear ratio (from 1^{st} to 6^{th} gear) [-]	14.94, 11.73, 9.04, 7.09, 5.54, 4.35
Gear ratio (from 7^{th} to 12^{th} gear) [-]	3.44, 2.7, 2.08, 1.63, 1.27, 1

3. Results and discussion

The implications of applying the different combinations of fuels and injector typologies proposed in this work are analysed by distinguishing three major aspects. First, the modifications on the injection settings and strategies necessary to maintain comparable and safe operating conditions on the engine. Then, the effect on the combustion process is presented based on the results obtained from the analysis of the heat release curves. Finally, the impact on emissions and fuel consumption is presented.

3.1. Injection Strategy

The injection strategy used for this work is based on the calibration presented in previous works on the DMDF concept [34]. This injection strategy is designed for using gasoline as LRF and diesel as HRF. At medium-low load conditions, early injections of the HRF ensure a premixed combustion, while the injection strategy moves near the TDC to promote a more diffusive combustion as the load is increased. In most part of the calibration map, a two-injection strategy is used to control the mixture stratification. By contrast, a single injection strategy is used at full load conditions, resulting in a more diffusive combustion [25].

When OMEx is used as the HRF, the injection strategy has to be modified due to changes in the LHV and reactivity of the fuel as compared to diesel. In general, longer injections are needed to introduce the same energy content in the cylinder, but changes in reactivity and duration of the injection alter the phasing of the combustion process. In order to keep the combustion process under comparable conditions, some modifications have to be done to the injection strategy. At low load conditions, where a more premixed combustion is desired, the pilot injection is kept the same, but the main injection has to be delayed as a consequence of the higher reactivity of OMEx. Even if

315 higher amount of fuel is injected, it burns faster, and it is necessary to delay the main
316 injection to still have an adequate phasing of the combustion. At medium load
317 conditions, a highly premixed combustion strategy is promoted. Under these conditions,
318 it is important to control the stratification degree through the pilot injection.
319 Considering that the higher cetane number of OMEx makes it more prone to auto ignite,
320 a fast premixed combustion with excessive pressure gradients can occur if the pilot fuel
321 injection is done too early in the compression stroke. The immediate solution to avoid
322 this issue is to reduce the premix degree of the fuel mixture by delaying the pilot
323 injection. At high load conditions, a single injection strategy is set to obtain a more
324 diffusive combustion. At these conditions, the reactivity of the mixture is of lesser
325 importance and the combustion rate is dominated by the mixing process, so the same
326 injection settings can be used independently of the fuel. For simplicity of the injection
327 strategy, when a double-injection strategy is used, the energizing time or time of
328 injection (TOI) is kept the same for both the pilot and the main injection.

329 The resultant injection settings are summarized in Table 6. As it can be checked, the
330 modifications needed when using OMEx as HRF are small enough to still have
331 comparable settings. These slight modifications were initially tested to ensure adequate
332 operation when using the injector with the lower mass flow capacity. In this way, the
333 settings can be kept the same when changing the injector, as the injector with the
334 highest mass flow capacity will not present problems of insufficient dwell time. The
335 energizing time reduction required when changing from the LFI to the HFI is also
336 included in Table 6. It can be seen that the TOI reduction needed to ensure that the
337 same amount of fuel is being injected is not proportional to the flow rate capacity of the
338 injector. This is dependent on the injection profile of each injector.

339 Table 6. Injection settings for the different fuels and hardware.

Operating Point	Diesel-Gasoline		OMEx-Gasoline		
	SOI (Pilot – Main) [CAD bTDC]	TOI (LFI – HFI) [μs]	SOI (Pilot – Main) [CAD bTDC]	TOI (LFI – HFI) [μs]	P rail [bar]
1	19 – 4	646 – 641	15 – 5	954 – 949	600
2	22 – 6	642 – 639	22 – 11	1123 – 1112	600
3	29 – 19	651 – 647	29 – 15	966 – 958	600
4	32 – 22	692 – 680	32 – 18	990 – 883	800
5	60 – 50	579 – 545	64 – 50	805 – 803	800
6	/ – 8	889 – 840	/ – 8	1514 – 1311	2000
7	/ – 7	1322 – 1149	/ – 7	2539 – 2082	2000
8	/ – 12	1095 – 1005	/ – 12	1929 – 1581	2000

340

341 The port fuel injection was tuned for each case with the objective of achieving the target
342 load (torque). Due to the differences in the mixing capabilities of the different high-
343 reactivity fuels and DI injectors, the port fuel injection must be tuned for each case to
344 compensate the change in the DI performance , thus changing substantially the gasoline
345 mass fraction (GF) and premixed energy ratio (PER) between the different cases.

$$GF = \frac{m_{LRF}}{m_{LRF} + m_{HRF}} \quad (2) \qquad PER = \frac{m_{LRF} \cdot LHV_{LRF}}{m_{LRF} \cdot LHV_{LRF} + m_{HRF} \cdot LHV_{HRF}} \quad (3)$$

346

347 The changes in PER for the different fuels and tested points are represented in Figure 5.
348 For the Diesel-Gasoline no significant impact on the engine performance was observed.
349 A slight increase in PER was necessary at higher loads, but no significant difference was
350 observed when changing the hardware. Contrary to this, the change of injector had a
351 major impact on injection performance when using the HRF with OMEx. For the
352 operating points with the large injections, a substantial decrease in performance
353 appeared and a higher amount of gasoline was necessary to be injected to achieve the
354 load targets. This change in the amounts of fuel will have an impact on fuel consumption
355 and engine performance as will be discussed in the following sections.

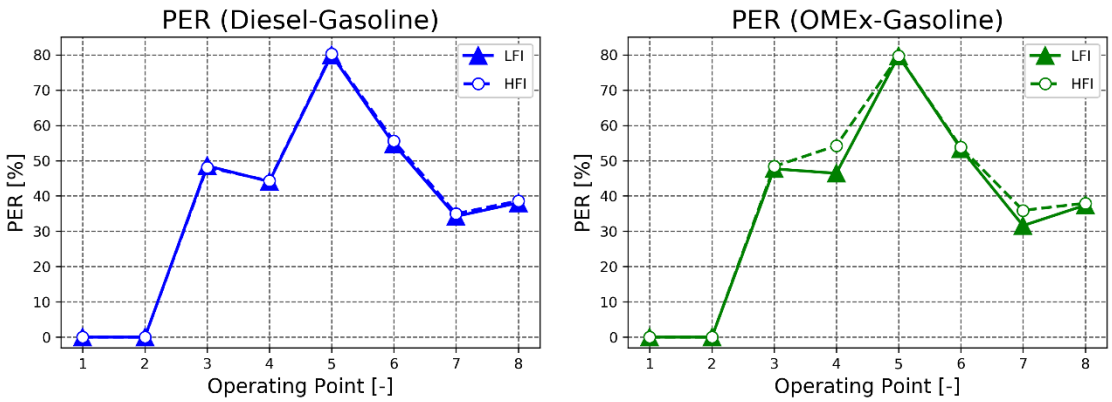

356 Figure 5. (a) PER values for each operating condition with Diesel-Gasoline and (b) with OMEx-Gasoline.

357

358 **3.2. Spray and Combustion performance**

359 The aforementioned changes in injection settings affect directly to both the reactivity
360 and homogeneity of the fuel mixture. Changes in PER when using the HFI (especially for
361 OMEx-Gasoline) imply a change in the properties of the fuel mixture like cetane number
362 or fuel equivalence ratio, therefore the ignition delay and the burning rate are affected.
363 For the studied cases, the changes in PER when comparing results from LFI and HFI can
364 be assumed to be negligible. Even for operating points 4 and 7 of the OMEx calibration,
365 the difference in PER is small enough to consider the effect of the fuel composition as a
366 second order effect. The use of the HFI also implies that the mixing capabilities of the
367 spray are different. The mixing rate of the spray will dictate the stratification level of the
368 in-cylinder mixture, and this will also affect the ignition delay and burning rate
369 depending on the operating point.

370 From Figure 6, a general trend can be observed in the CA10. When comparing the results
371 from the LFI and HFI, the differences in CA10 can be interpreted as differences in the
372 effective ignition delay. For the operating points studied, all cases show that the HFI
373 produces a more delayed start of combustion.

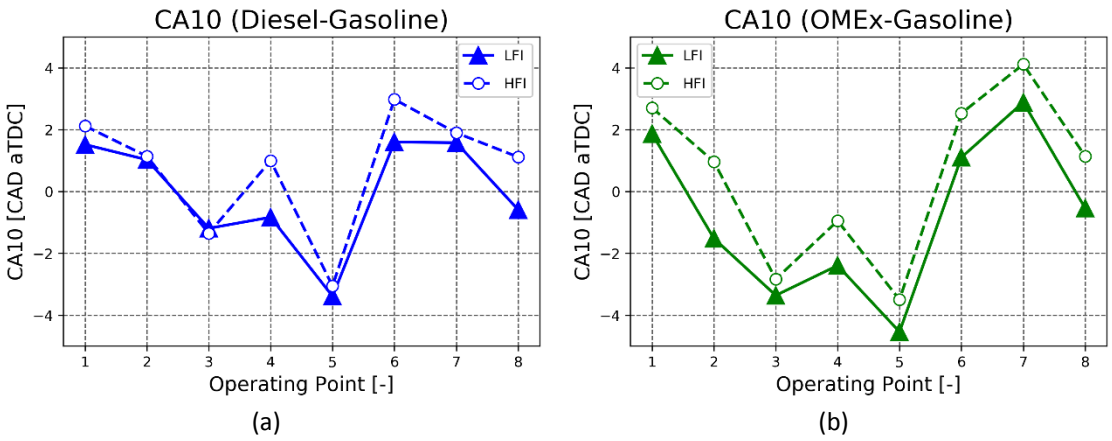

Figure 6. (a) CA10 values for each operating condition with Diesel-Gasoline and (b) with OMEx-Gasoline.

Starting with the Diesel cases, there is a clear distinction between the premixed and diffusive operating points. When the combustion mode is premixed, there is almost no difference between the results of the HFI and LFI (points 2 and 3, for example). This means that both injectors have been able to produce similar levels of stratification before the start of combustion. For the more diffusive operating conditions (points 6, 7 and 8, for example), the ignition occurs before the end of the injection. This means that a purely diffusive flame takes place and the ignition delay and burning rate are defined by the mixing rate. The HFI will produce higher fuel concentration levels and will take more time to achieve an air-fuel ratio inside the flammability limits.

The same explanation applies to the cases with OMEx, but an additional effect must be considered due to the change in composition of the fuel being injected. The change in the fuel composition can affect the ignition delay differently depending on the combustion regime. If the in-cylinder charge is completely homogeneous before the start of combustion, the only difference is due to the chemical composition, which can be compared through the cetane number. Comparing Figure 6a and Figure 6b, it can be observed that OMEx produces shorter ignition delays at points where the premixing level is high, mainly due to this reason. For diffusive flames, two effects can be

considered to understand the difference in the ignition delay: evaporation and mixing. The evaporation and mixing rates are scaled according to certain physical properties of the fuel, but the time required for the process is proportional to the amount of fuel mass, that has been scaled with the LHV to maintain the energy input when changing fuels. According to this, a very simple comparison can be done based on proportionality. These proportionalities of the evaporation and mixing rates can be obtained either form thermofluid-dynamic theories or from various simplified models for inert sprays available in the literature [42].

$$t_{evap} \propto m_f, \frac{1}{P_{vap}} \rightarrow \frac{t_{evap,D}}{t_{evap,OMEx}} \approx \frac{\frac{m_D}{P_{vap,D}}}{\frac{m_{OMEx}}{P_{vap,OMEx}}} \approx \frac{\frac{LHV_D}{P_{vap,D}}}{\frac{LHV_{OMEx}}{P_{vap,OMEx}}} \approx 1 \quad (4)$$

$$t_{mix} \propto \frac{\mu_a}{\mu_f}, \frac{\rho_f}{\rho_a}, m_f \rightarrow \frac{t_{mix,D}}{t_{mix,OMEx}} \approx \frac{\frac{\rho_D}{\mu_D}}{\frac{\rho_{OMEx}}{\mu_{OMEx}}} \cdot \frac{m_D}{m_{OMEx}} \approx \frac{\frac{\rho_D}{\mu_D}}{\frac{\rho_{OMEx}}{\mu_{OMEx}}} \cdot \frac{LHV_D}{LHV_{OMEx}} \approx 0.1 \quad (5)$$

From Equation (4), it can be concluded that the evaporation process does not include any remarkable difference between diesel and OMEx. In this sense, even though OMEx evaporates at a faster rate, the fact that a higher amount of fuel mass has to be evaporated means that similar evaporation times will be achieved with both fuels. On the other hand, Equation (5) shows that the mixing process presents a more significant difference. Particularly, OMEx will take longer time to mix and will result in a longer ignition delay. This simplified comparison is consistent with the results obtained from experiments, and even if it does not include effects like turbulence or complex flows inside the cylinder, it is enough to justify the differences appreciated between both fuels without resorting to complex and time-consuming CFD simulations.

411 From this brief analysis, a derived conclusion can be extracted for the results with OMEx.
412 A significant difference in the ignition delay can be observed between the LFI and the
413 HFI in the operating points where a premixed combustion is promoted (points 1 to 3).
414 The expected result for these points was that no significant difference would be
415 appreciated (as happens with diesel), but that is not the case. This can be interpreted as
416 a limitation of the mixing capabilities of the injector due to a combination of longer
417 injections and lower mixing capabilities of the fuel. The HFI produces higher
418 concentrations of fuel, and they will take longer to mix and achieve conditions inside the
419 flammability limits of the fuel.

420 In order to support this statement, a set of one-dimensional simulations were carried
421 out to have a better understanding of the morphology of the spray with the different
422 injector geometries and the different fuels. For these simulations the in-house software
423 DICOM was used, as it allows to have into account the thermodynamic evolution inside
424 the cylinder, as well as the differences in the injection rate [44][45]. For the four sets of
425 results, the same operating condition was used to evaluate the spray evolution.
426 Operating point 7 was selected as it is where longer injections and later ignition occur.
427 The in-cylinder thermodynamic evolution before combustion is almost identical for the
428 four cases, so an average pressure and temperature was used to perform the evaluation
429 under the same conditions. The results from the simulations are most reliable before
430 combustion, but this is not a big limitation as ignition (CA10) occurs in a relatively narrow
431 gap in CAD for the four cases. Figure 7 represents the injection profiles as well as the in-
432 cylinder pressure and temperature used for the simulations. It can be appreciated the
433 difference in the maximum flow capacity of the two injectors, as well as the effect in the
434 fuel density. Also, the injection duration reduction can be appreciated to be

considerable when using the HFI. In Figure 7 it is designed with a light grey color the region up to which the comparison between the different spray morphologies is valid, and with a darker grey the region where combustion is taking place and the simulations are not reliable nor comparable. Notice that ignition occurs before any of the injections has finalised and makes more obvious the predominance of the diffusive combustion at higher loads.

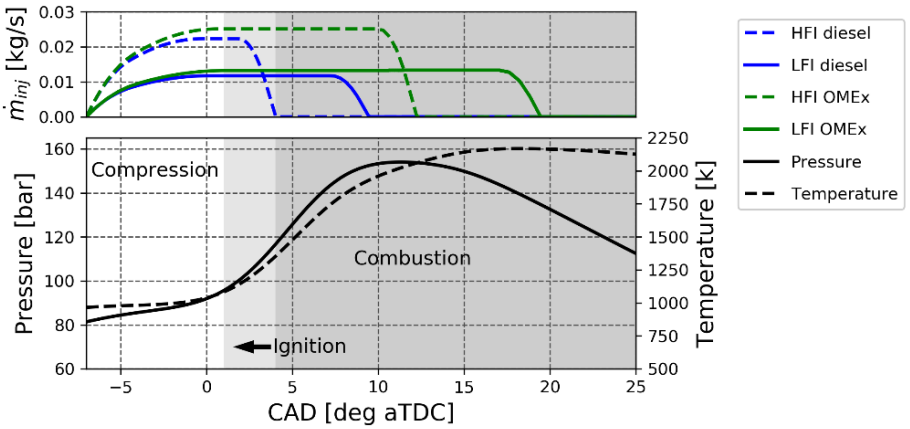

Figure 7. Injection profile and thermodynamic evolution used to simulate the spray transient evolution

To evaluate the injection and mixing capacity of each injector it is possible to evaluate the spray tip penetration. In Figure 8 the results for the four cases, represented in solid color until reaching their correspondent CA10, the limit of this comparison. The results show a clear tendency in which the HFI has a higher flow velocity at the orifice and is able to have a higher penetration capacity. This is associated with a lower capacity to diffuse fuel in air, and the momentum is being dissipated slower. Also, OMEx presents a slightly better mixing capacity than diesel as a consequence of the balance between density, viscosity and mass flow rate [42].

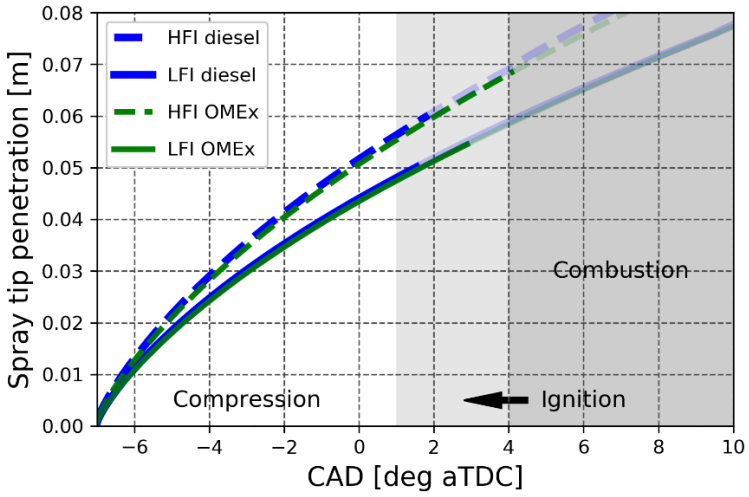

Figure 8. Spray tip penetration during injection before combustion

To evaluate the effect of this difference in mixing capacity, in Figure 9 the stratification of the spray is represented trough the mass fraction of fuel at different equivalence ratio. Figure 9a corresponds to the instant where autoignition occurs for the LFI with diesel, and Figure 9b corresponds to the instant when OMEx ignites with the LFI. These two instants show the same tendency for both fuels: the LFI produces higher concentrations at lean equivalence ratios and lower concentrations at rich equivalence ratios that the HFI for the same instant of injection. This means that while the LFI produces a more diluted mixture able to ignite, the HFI produces higher concentrations of fuel that need more time to mix and reach a condition where autoignition can occur. Between the two fuels there is an important difference to consider before attempting to compare both representations (despite representing to different instants), and it is the difference in stoichiometric air-to-fuel ratio (AF_{st}). While diesel has an AF_{st} of approximately 15, OMEx has a much lower AF_{st} of 7.8, meaning that with lower entrained air can reach leaner conditions. This explains the significant difference in mass fractions and average equivalence ratio between the two fuels. Additionally, the effect of the LFR that stratifies the AF_{st} of the mixture inside the cylinder has not been

considered in this representation with the intention of evaluating the spray properties of the different hardware. If this effect is considered, the results with OMEx would move towards richer conditions.

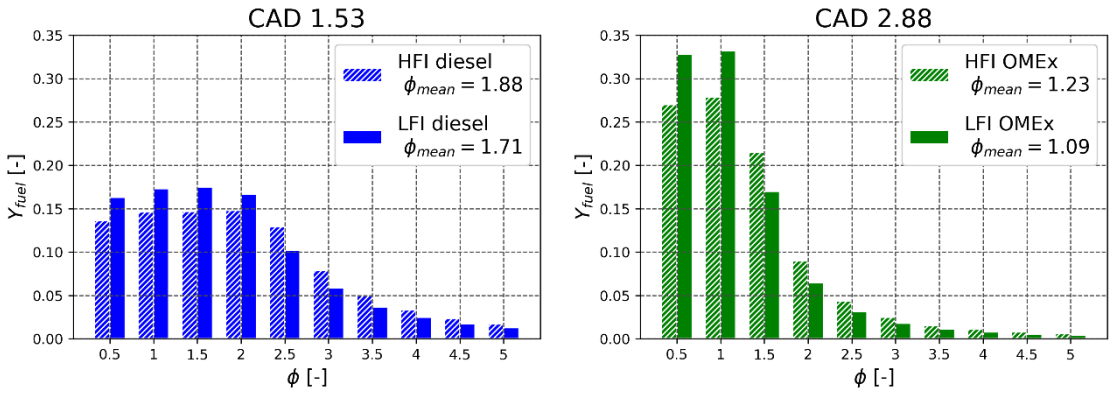

(a) (b)

Figure 9. (a) Fuel stratification inside the Diesel spray and (b) the OMEx spray.

The next parameter to consider for combustion performance is the CA50, related to the combustion phasing. The results for this parameter are shown in Figure 10. The results observed for combustion phasing show a clear change of tendency when moving to a more diffusive combustion (points 6 to 8). A slight delay of the CA50 is observed for the HFI due to the delayed ignition. In the case of OMEx, the difference is even lower due to the higher reactivity of the fuel that accelerates the burning rate compared to diesel. For the more premixed cases, the burning rate is a process more influenced by chemical kinetics, not only by mixing, and this kinetic rate is affected by the turbulence levels and local stratification. These complex effects are responsible for the greater variation of the CA50, but there is a consistent tendency to have a delayed combustion phasing when using the HFI as a derived consequence of having a delayed ignition.

Despite the changes in combustion phasing, no significant impact was observed in engine performance (power output) or specific fuel consumption except for the slight

increase in the PER required for operating points 4 and 7 when using OMEx. This topic will be further addressed in the following section.

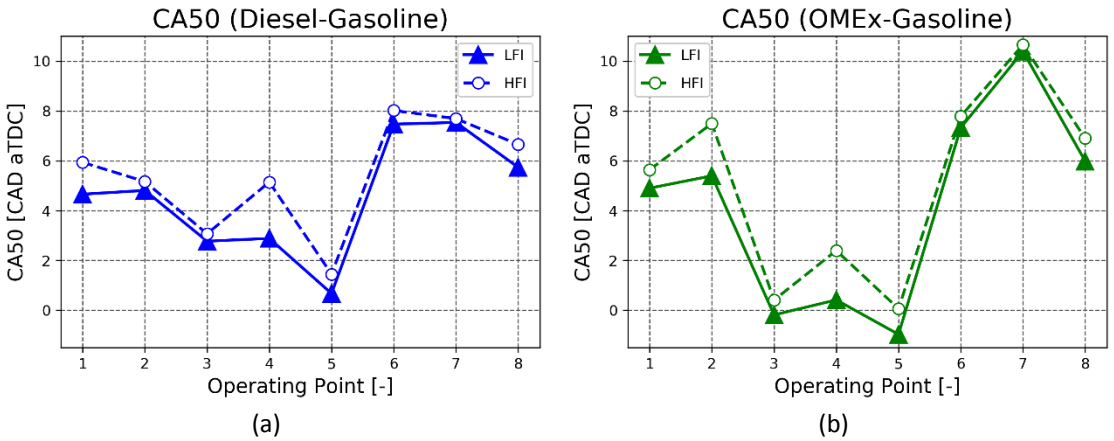

Figure 10. (a) CA50 values for each operating condition with Diesel-Gasoline and (b) with OMEx-Gasoline.

The same reasoning used to explain the results and differences in combustion phasing (CA50) can be extended to the combustion duration (CA90-CA10), but in this case the reactivity of the fuel mixture takes a greater relevance. As seen in Figure 11, for both fuels, there is an increase of combustion duration when using the HFI compared to the LFI in the operating points with a more premixed combustion. As explained before, this is because of the prevalence of kinetic rates combined with three-dimensional effects like turbulence and fuel stratification. When going to a more diffusive combustion, a difference in tendencies appears between the two fuel combinations. This difference is consequence of the balance of two main effects: reactivity and mixing rate. As the HRF mixes with the LRF and the air inside the cylinder, the reactivity of the mixture increases, and the fuel is burnt faster. When using the HFI, the ignition delay cannot be compensated with the increase in reactivity and the combustion continues further during the expansion stroke and results to be longer. For OMEx, the scenery is different. Due to the higher reactivity and the lower stoichiometric air-to-fuel ratio compared to diesel, the more the HRF and LRF mix, the lower the global AF. With the lower AF and

higher reactivity, the burning rate is enhanced, which accelerates the heat release and actuates as an enhancer of mixing.

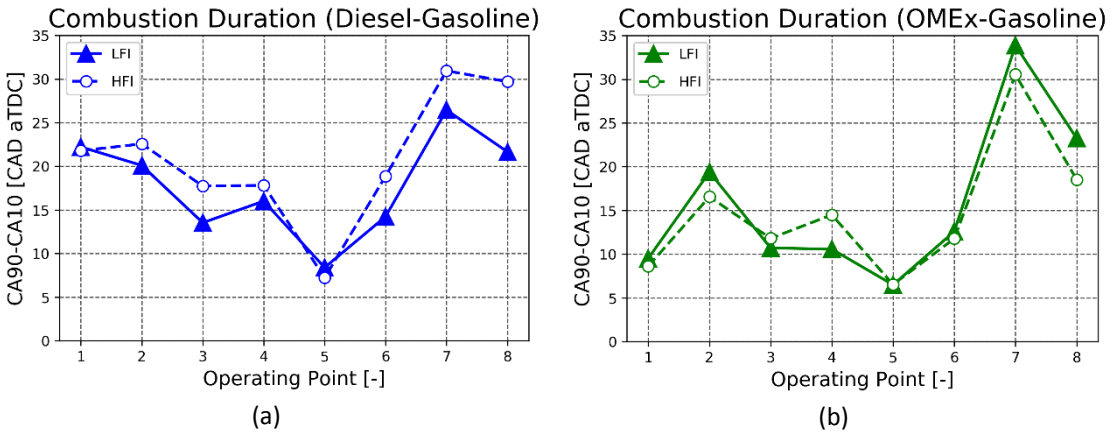

Figure 11. (a) Combustion duration for each operating condition with Diesel-Gasoline and (b) with OMEx-Gasoline.

Figure 12 and Figure 13 show the RoHR profiles for the different operating points for Diesel and OMEx, respectively. For both fuel combinations, a clear premixed combustion can be appreciated for the operating points up to 50% load. Under high load conditions it is noticeable that a staged combustion appears. In the case of OMEx, the later stage of combustion clearly corresponds with a diffusive combustion as a consequence of the excessively long injection times. In the case of diesel injections, the end of the direct injection and the start of the last combustion stage overlap, which makes difficult to determine if the staged combustion is driven by the diffusion process of the highly concentrated fuel regions coming from the injection process or if it is a late combustion coming from the stratified mixture where regions with different cetane number are formed and some of them can burn later. To confirm which case is taking place it would be necessary to have optical access to the combustion chamber and directly measure the driving phenome or use high fidelity 3D CFD. Both options are beyond the scope of this work. In the case of OMEx a very clear change of slope is appreciated in those cases where the change in reactivity of the fuel mixture is significant.

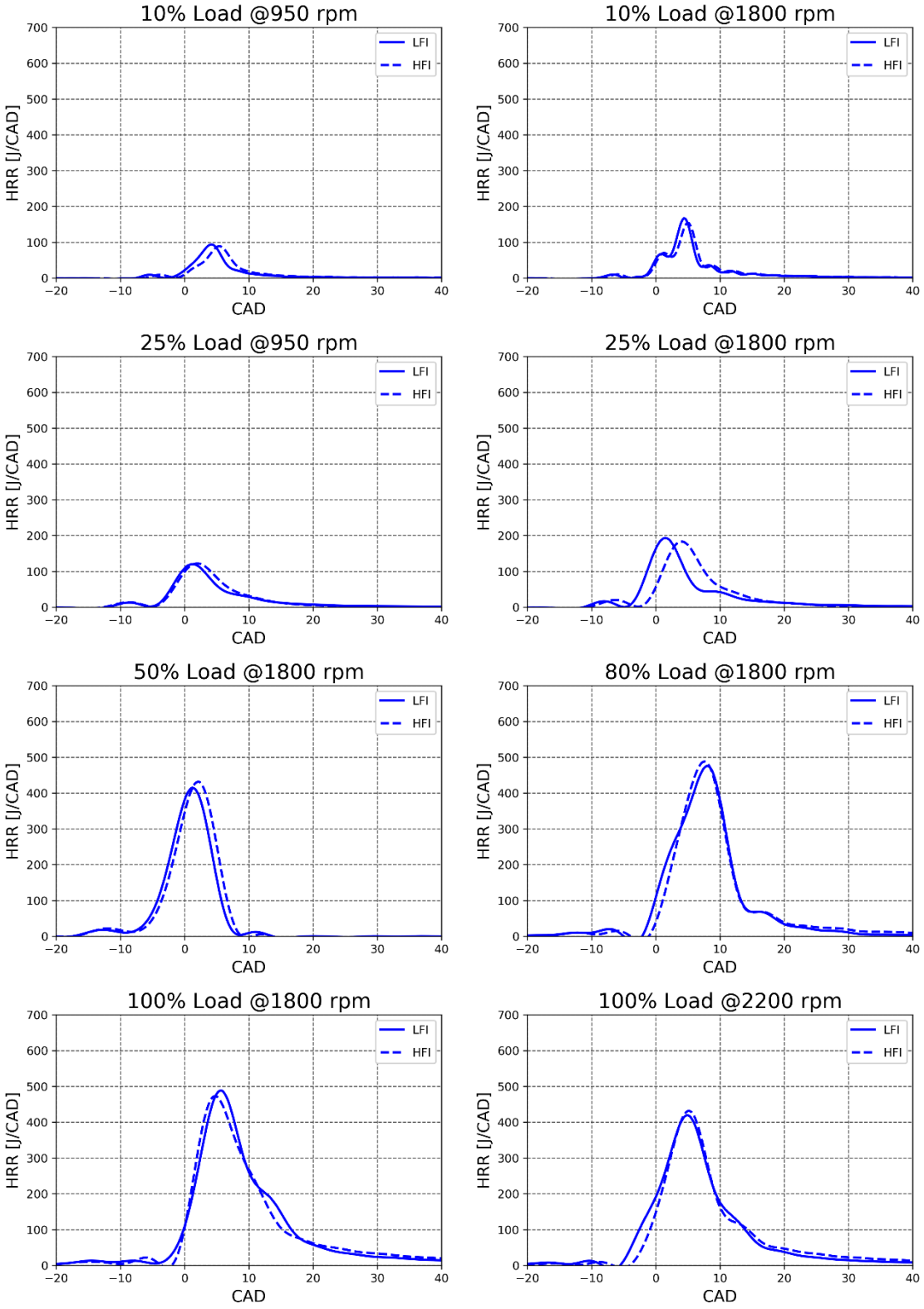

523 Figure 12. Heat release of every operating point for Diesel-Gasoline DMDF with LFI and HFI

524

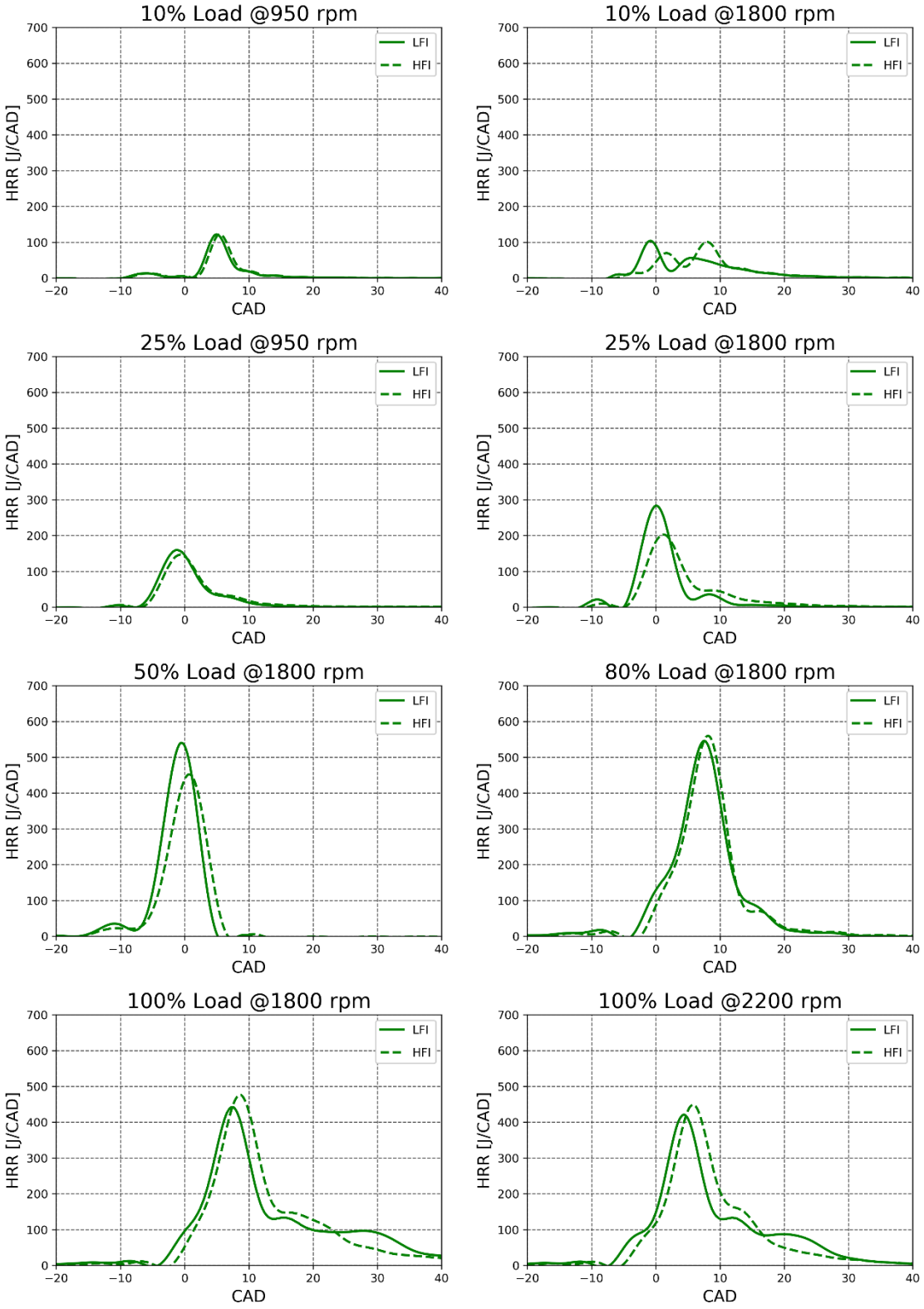

525 Figure 13. Heat release of every operating point for OMEx-Gasoline DMDF with LFI and HFI

3.3. Engine performance and emissions results

Figure 14 shows the equivalent brake specific fuel consumption ($BSFC_{eq}$) for both diesel-gasoline and OMEx-gasoline. As shown in Equation (6)), the equivalent BFSC takes into account the differences in LHV between the different fuels and considers the diesel fuel as reference to maintain the same energy basis for all the mixtures. Then, it is possible to decouple the effects of the different LHV from the differences on the combustion process. In Figure 14, it can be appreciated that the use of the HFI has a detrimental impact on the specific fuel consumption in general, but the increase is small enough to justify that there is no difference in fuel consumption independently of the hardware used. This enforces the previous conclusion that the change in combustion phasing is small enough to not have an impact on the performance of the engine.

$$BSFC_{eq}[g/kWh] = \frac{\dot{m}_{HRF} \cdot \left(\frac{LHV_{HRF}}{LHV_{diesel}}\right) + \dot{m}_{LRF} \cdot \left(\frac{LHV_{LRF}}{LHV_{gasoline}}\right)}{Torque} \quad (6)$$

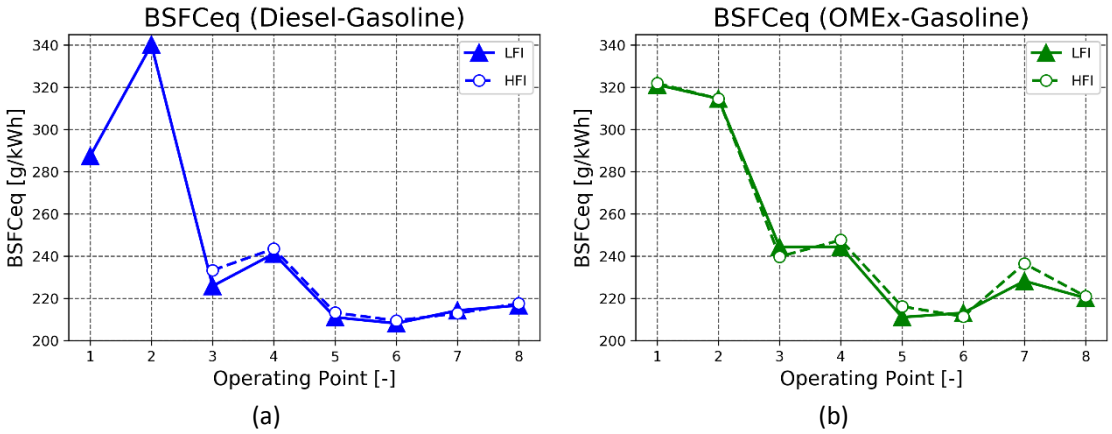

Figure 14. (a) Equivalent BSFC values for each operating condition with Diesel-Gasoline and (b) with OMEx-Gasoline.

In terms of NOx emissions, a clear effect appears for Diesel when using the HFI. The higher equivalence ratio of the mixture during the combustion process produces higher temperatures, which lead to a higher NOx production. As seen in Figure 15, the use of the LFI allows to reach the Euro 6 NOx limit (0.4 g/kWh [46]) in most of the operating

points. The use of the HFI produces higher NOx emissions in almost all the operating conditions in the case of diesel. By contrast, no clear differences can be appreciated in the case of OMEx, with some points producing lower while other higher NOx than the LFI. In this sense, it can be concluded that the low LHV and the low stoichiometric AF of the OMEx allow to have low-temperature flames independently of the mixing capabilities of the hardware.

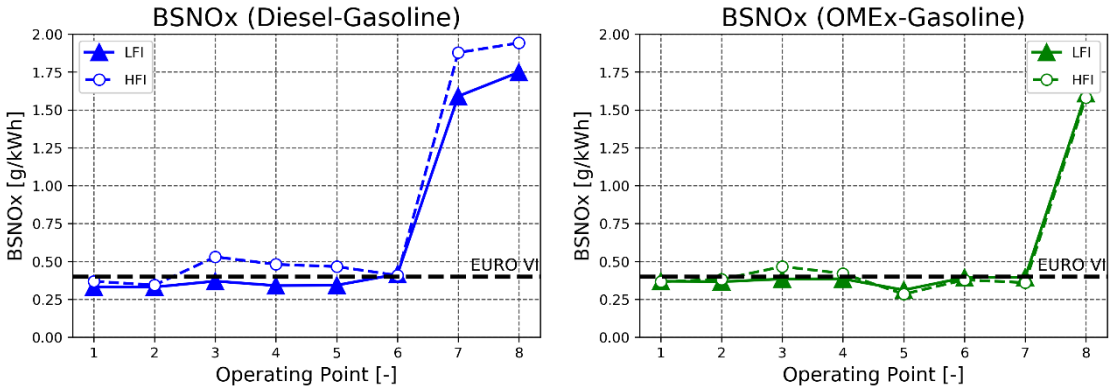

Figure 15. (a) BSNOx values for each operating condition with Diesel-Gasoline and (b) with OMEx-Gasoline.

Figure 16 and Figure 17 show the results in terms of BSCO and BSHC emissions. In terms of CO emissions, no clear difference can be observed. By contrast, a consistent increase of unburnt hydrocarbons appears when the HFI is used. The main source of these contaminants is the fuel fraction trapped in the piston clearances and crevices during compression (mainly coming from the LRF introduced through PFI). Seeing how the CO fraction remains considerably unaltered, it can be deduced that the fraction of fuel trapped inside the crevices is more or less the same, and the chemical equilibrium of CO formation is reached independently of the injector employed. When including the HC emissions results to this conclusion, there is an additional source of HC. The other main source of HC is from the incomplete combustion of the fuel, therefore, there is a systematic drop of combustion efficiency when using the HFI because of the poor mixing

performance. When the resultant levels of these emissions are compared to the limit values imposed in the Euro 6 legislation (1.5 g/kWh for BSCO and 0.13 g/kWh for BSHC [46]), any of the operating points fulfils the requirements. This is a clear problem for the DMDF combustion mode, but it can be easily solves incorporating a DOC in the aftertreatment system (ATS) that would oxidize these substances to complete combustion [47].

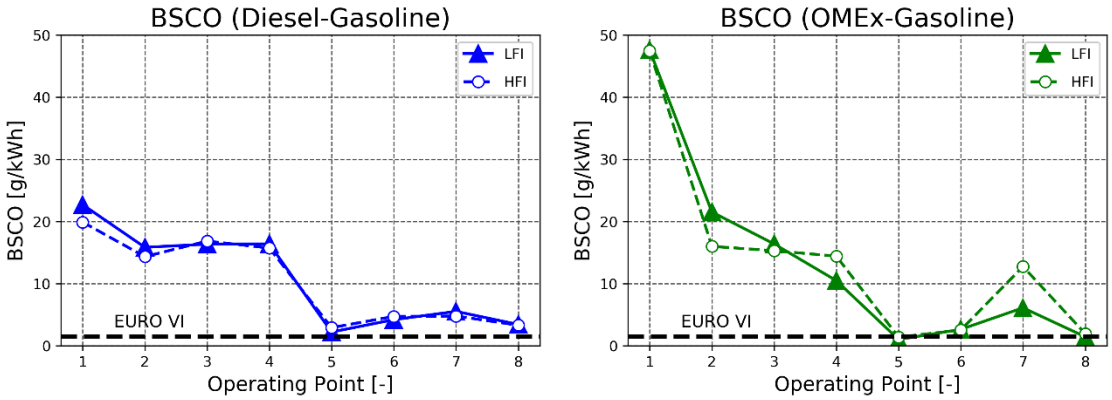

Figure 16. (a) BSCO values for each operating condition with Diesel-Gasoline and (b) with OMEx-Gasoline.

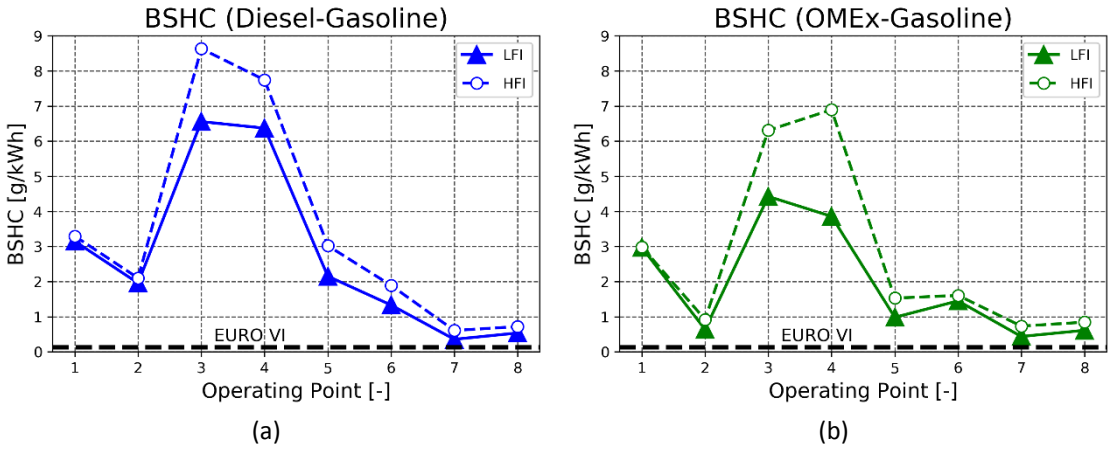

Figure 17. (a) BSHC values for each operating condition with Diesel-Gasoline and (b) with OMEx-Gasoline.

Finally, Figure 18 shows that the soot production is enhanced at high load conditions for the diesel cases due to a diffusive combustion under richer conditions. The soot

production at high loads greatly surpasses the limit of 0.01 g/kWh imposed by the Euro 6 normative. By contrast, OMEx showed zero soot emissions independently on the hardware used. This is one of the main benefits of OMEx that has already been reported in the literature that makes it so interesting for its application in a DMDF combustion mode [34] .

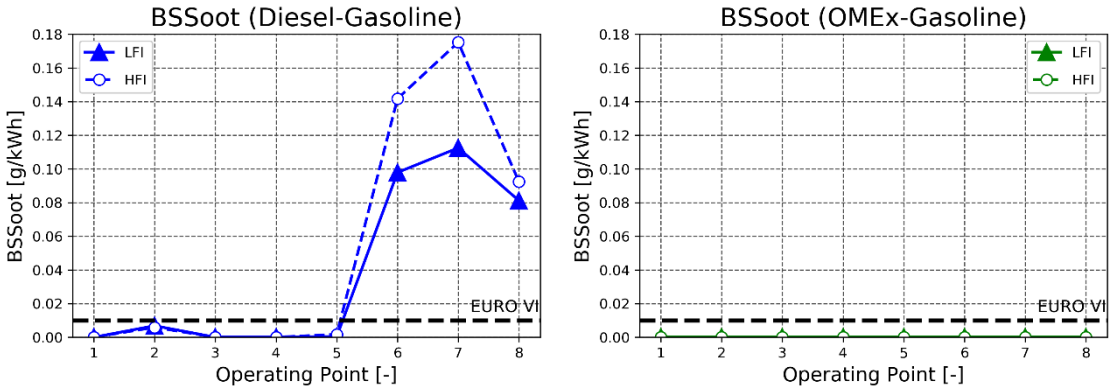

Figure 18. (a) BSSoot values for each operating condition with Diesel-Gasoline and (b) with OMEx-Gasoline.

4. Selection of best hardware

The experimental results show a consistent behaviour for both injectors. In general, the LFI performs better in terms of emissions, but slight benefits in CO or NOx (only for OMEx) emissions can be observed at certain points when using the HFI. In order to evaluate the global benefit or worsening of each injector the following methodology will be used: the first step is to simulate a real condition of engine operation. With the whole operation of the engine, the different operating states will be correlated to the experimental points measured in this work to evaluate the representativeness of the measured operating conditions and give each operating point a weight in the driving cycle. The engine performance during the driving cycle will be computed as the weighted

592 average of the results from the experimental measurements. Finally, a merit function
593 will be used to determine which is the best hardware to use.

594 To produce the operating points of the engine during real driving conditions, a complete
595 map of the DMDF engine was used to implement in a vehicle simulation using the
596 software GT-Suite [48]. For this simulation, a homologation driving cycle WHVC was
597 imposed on a heavy-duty vehicle with a payload of 50% of its maximum cargo as
598 established by the standard procedure [46]. This simulation is limited to stationary
599 points and does not include transient effects, but it is more than enough to evaluate the
600 real performance of the engine. In Figure 19 are included all the operating points in
601 which the engine must operate during the WHVC with a constant time step of 0.1
602 seconds between them. Based on the number of points and the BSFC, a representative
603 region is assigned to each of the eight points measured in this work in such a way that
604 the weighted average BSFC of the region has a difference of less than 3% of BSFC with
605 the experimental point [50]. This routine is only performed once as for all fuels and
606 hardware, the power output map is the same, therefore the driving cycle will result in
607 the same scatter of operating points. The representative regions of each point are also
608 included in Figure 19. A summary of the weight of each operating point is included in
609 Table 7. As not all the points are covered by the eight measured operating points, the
610 global weight of each point is normalized by the total number of represented points in
611 order to have a coherent average value of fuel consumption and emissions. The whole
612 simulation consisted of 11109 points, and the 8 measured points can cover

approximately 80% of these operating conditions. With this, it can be assured that the results from this analysis are representative of the complete driving cycle.

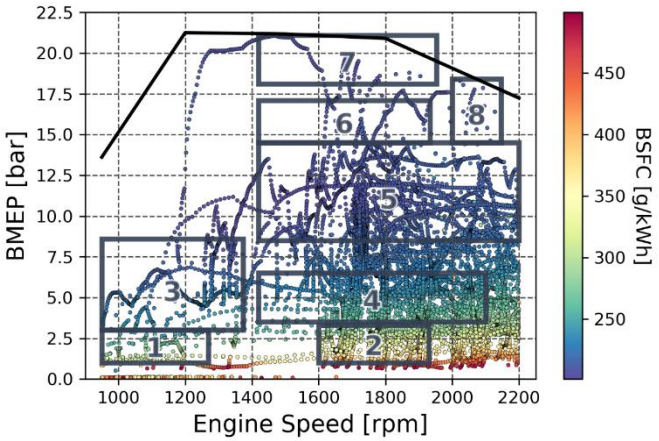

Figure 19. Engine operating conditions during WHVC driving cycle and representative region of the measured operating points

Table 7. Summary of the representativeness of each measured point during a driving cycle.

Operating Point	Number of points	Percentual Weight [%]	Normalized percentual weight [%]
Complete simulated driving cycle	11109	100	-
1	182	1.64	2.06
2	731	6.58	8.29
3	592	5.33	6.71
4	3524	31.72	39.97
5	3534	31.81	40.08
6	160	1.44	1.81
7	72	0.65	0.82
8	22	0.20	0.25
Total	8817	79.37	100.00

The representative averages for each case obtained with the normalized weight for each point are included in Table 8. In general, the HFI produces more emissions with a higher specific fuel consumption. The drop in engine efficiency when using the HFI increases the BSFC and the only emission constrain that fulfils with diesel is the soot limitation.

To better quantify how much the engine performance is deteriorated when using the HFI with each fuel, a merit function is used. Considering this particular application in which CO and HC emissions could be removed with the use of a single DOC adapted to specifically work with OMEx emissions that results in a relatively simple ATS [51], these contaminants can be of lesser relevance as engine-out emissions, and the fuel consumption does not show great variations between cases, therefore the most relevant performance parameters to evaluate are NOx and soot emissions [52]. For this case it is recommended in the literature to use the multi-objective merit function written in Equation (7), where the subscript "t" refers to the objective or reference value to evaluate each performance parameter [53].

$$F = \left(\left(\frac{BSNOx}{BSNOx_t} \right)^2 + \left(\frac{BSSoot}{BSSoot_t} \right)^2 \right)^{0.5} + \frac{BSCO}{3 \cdot BSCO_t} + \frac{BSHC}{3 \cdot BSHC_t} + \frac{BSFC_{eq}}{3 \cdot BSFC_{eq,t}} \quad (7)$$

The target values for the emissions are the limits established by the norm Euro 6 that have already been mentioned: 0.4 g/kWh for BSNOx, 1.5 g/kWh for BSCO, 0.13 g/kWh for BSGC and 0.01 g/kWh for BSSoot [46]. For the reference value of the fuel consumption it has been decided to use the minimum value from all points in each set. In this way, it is possible to include how much the average BSFC of the complete engine operation is increased relative to its best performance condition. In fact, the minimum values of $BSFC_{eq}$ are very similar for all the cases and the comparison can be expanded to all the combinations of fuel and hardware. The values obtained for the merit function (F) are also included in Table 8.

The values of the merit function F denote that the lower the value the better the engine performance. Two main conclusions can be extracted from this analysis: the first

conclusion is that the HFI has an overall worse performance than the LFI, therefore the LFI is a better option for low-emissions applications. The second conclusion that can be extracted is that the benefits of OMEx in terms of emissions surpasses by far the slight increase in specific fuel consumption, and makes this fuel a very promising candidate as an alternative fuel for the future of low-emissions internal combustion engines.

Table 8. Summary of results for a driving cycle for each combination of fuel and hardware.

	$BSFC_{eq}$ [g/kWh]	BSNOx [g/kWh]	BSCO [g/kWh]	BSHC [g/kWh]	BSSoot [g/kWh]	F [-]
Diesel LFI	236.37	0.36	10.45	4.10	0.0036	14.14
Diesel HFI	238.66	0.48	10.32	5.17	0.0054	17.24
OMEx LFI	237.69	0.36	8.56	2.38	0.0000	9.26
OMEx HFI	240.78	0.37	9.81	3.97	0.0000	13.65

5. Conclusions

This study investigated the suitability of different injector typologies for the use of e-fuels with low LHV in the dual-mode dual-fuel combustion concept with the objective of selecting the most suitable injector. The investigation was carried out using a multi-cylinder 8L production engine modified to promote the dual-fuel combustion. Moreover, two different fuel combinations were studied, diesel-gasoline and OMEx-gasoline. The results of this investigation showed that:

- The use of low LHV fuels requires an adaptation of the injection strategy for longer injections in order to maintain equivalent energy inputs.
- The use of injectors with high flow capacity result in a delayed ignition that could be overcome with a recalibration of the injection strategy.
- The mixing capability depends on both the injector and fuel properties. In general, high flow injectors show lower mixing capabilities resulting in a generally delayed combustion phasing and narrow margin for the injection

calibration. Too early injections result in too strong premixing with high pressure gradients and too late injections result in a decrement of power output.

- For the tested operating points, the change in combustion phasing did not affect the equivalent specific fuel consumption.
- NOx, soot and unburned hydrocarbons emissions were increased when using the injector with higher flow capacity as a consequence of too rich combustion and a worsening of the combustion efficiency.
- Under real driving conditions, the high flow injector with diesel is not able to fulfil Euro 6 normative for NOx and soot.
- Global performance results show that the low flow injector is the best option for low-emission applications.
- OMEx capabilities for low-NOx and zero-soot emissions far compensate the increase in specific fuel consumption and highlight its benefits as a candidate for the fuel of the future.

From these results, it can be concluded that the use of high flow capacity injectors for low LHV fuels is capable of solving the problem of too long injections, but the mixing capability is compromised and it affects the combustion process negatively. While the low flow capacity injectors are limited by the injection duration, they allow for a more flexible injection strategy and reduce emissions while fulfilling the performance targets.

Acknowledgments

The authors thanks VOLVO Group Trucks Technology and ARAMCO Overseas Company for supporting this research. The authors also acknowledge FEDER and Spanish Ministerio de Economía y Competitividad for partially supporting this research through

TRANCO project (TRA2017-87694-R) and the Universitat Politècnica de València for partially supporting this research through Convocatoria de ayudas a Primeros Proyectos de Investigación (PAID-06-18).

References

[1] McKinsey & Company. (2019). Global Energy Perspective 2019: Reference Case. In Energy Insights (Issue January). https://www.mckinsey.com/industries/oil-and-gas/our-insights/global-energy-perspective-2019. Accessed in December, 2019.

[2] Kalghatgi, G. (2018). Is it really the end of internal combustion engines and petroleum in transport? Applied Energy, 225(February), 965–974. https://doi.org/10.1016/j.apenergy.2018.05.076

[3] Verhelst, S., Turner, J. W., Sileghem, L., & Vancoillie, J. (2019). Methanol as a fuel for internal combustion engines. Progress in Energy and Combustion Science, 70, 43–88. https://doi.org/10.1016/j.pecs.2018.10.001

[4] Kalghatgi, G. (2019). Development of Fuel/Engine Systems — The Way Forward to Sustainable Transport. Engineering, 5(3), 510–518. https://doi.org/10.1016/j.eng.2019.01.009

[5] Erbach, G. (2018). BRIEFING: EU Legislation in Progress: CO_2 emission standards for heavy-duty vehicles (Issue August). https://www.europarl.europa.eu/RegData/etudes/BRIE/2018/628268/EPRS_BRI(2018)628268_EN.pdf. Accessed in April, 2019.

[6] D. Miller, J., & Façanha, C. (2014). THE STATE OF CLEAN TRANSPORT POLICY A 2014 SYNTHESIS OF VEHICLE AND FUEL POLICY DEVELOPMENTS. www.theicct.org/state-of-clean-transport-policy-2014 . Accessed in 12, January, 2020.

[7] Fontaras, G., Zacharof, N.-G., & Ciuffo, B. (2017). Fuel consumption and CO_2 emissions from passenger cars in Europe – Laboratory versus real-world emissions. Progress in Energy and Combustion Science, 60, 97–131. https://doi.org/10.1016/j.pecs.2016.12.004

[8] Zhang, W., Bange, M., Bohemer, S., Khair, M., & Tan, J. (2013). Electric heating assisted passive and active regeneration for efficient emission controls of diesel engines (Patent No. US 2013/0213010 A1). https://patents.google.com/patent/US9708945

[9] Terdich, N., & Martinez-Botas, R. (2013). Experimental efficiency characterization of an electrically assisted turbocharger. SAE Technical Papers, 6. https://doi.org/10.4271/2013-24-0122

[10] Luján, J. M., Bermúdez, V., Dolz, V., & Monsalve-Serrano, J. (2018). An assessment of the real-world driving gaseous emissions from a Euro 6 light-duty diesel vehicle using a portable emissions measurement system (PEMS). Atmospheric Environment, 174(November 2017), 112–121. https://doi.org/10.1016/j.atmosenv.2017.11.056

[11] Zhao, H. (2010). Advanced direct injection combustion engine technologies and development. Woodhead Publishing Limited. https://doi.org/10.1533/9781845697327

[12] Breakthrough: new Bosch diesel technology provides solution to NOx problem. Available in https://www.bosch-presse.de/pressportal/de/en/breakthrough-new-bosch-diesel-technology-provides-solution-to-nox-problem-155524.html. Accessed in April, 2019.

[13] Benajes, J., Martín, J., García, A., Villalta, D., & Warey, A. (2017). Swirl ratio and post injection strategies to improve late cycle diffusion combustion in a light-duty diesel engine. Applied Thermal Engineering, 123, 365–376. https://doi.org/10.1016/j.applthermaleng.2017.05.101

[14] López, J. J., Martín, J., García, A., Villalta, D., & Warey, A. (2017). Implementation of two color method to investigate late cycle soot oxidation process in a CI engine under low load conditions. Applied Thermal Engineering, 113, 878–890. https://doi.org/10.1016/j.applthermaleng.2016.11.095

[15] Olmeda, P., García, A., Monsalve-Serrano, J., & Lago Sari, R. (2018). Experimental investigation on RCCI heat transfer in a light-duty diesel engine with different fuels: Comparison versus conventional diesel combustion. Applied Thermal Engineering, 144(June), 424–436. https://doi.org/10.1016/j.applthermaleng.2018.08.082

[16] Reitz, R. D., & Duraisamy, G. (2015). Review of high efficiency and clean reactivity controlled compression ignition (RCCI) combustion in internal combustion engines. Progress in Energy and Combustion Science, 46, 12–71. https://doi.org/10.1016/j.pecs.2014.05.003

[17] Martins, M., Fischer, I., Gusberti, F., Sari, R., & Nora, M. D. (2017). HCCI of Wet Ethanol on a Dedicated Cylinder of a Diesel Engine. SAE Technical Papers, 2017-March(March). https://doi.org/10.4271/2017-01-0733

[18] Weall, A., Szybist, J. P., Edwards, K. D., Foster, M., Confer, K., & Moore, W. (2012). HCCI Load Expansion Opportunities Using a Fully Variable HVA Research Engine to Guide Development of a Production Intent Cam-Based VVA Engine: The Low Load Limit. SAE International Journal of Engines, 5(3), 2012-01–1134. https://doi.org/10.4271/2012-01-1134

[19] Benajes, J., Molina, S., García, A., & Monsalve-Serrano, J. (2015). Effects of low reactivity fuel characteristics and blending ratio on low load RCCI (reactivity controlled compression ignition) performance and emissions in a heavy-duty diesel engine. Energy, 90, 1261–1271. https://doi.org/10.1016/j.energy.2015.06.088

[20] Benajes, J., Molina, S., García, A., & Monsalve-Serrano, J. (2015). Effects of direct injection timing and blending ratio on RCCI combustion with different low reactivity fuels. Energy Conversion and Management, 99, 193–209. https://doi.org/10.1016/j.enconman.2015.04.046

[21] Pedrozo, V. B. (2017). An experimental study of ethanol-diesel dual-fuel combustion for high efficiency and clean heavy-duty engines [Brunel University of London]. http://bura.brunel.ac.uk/handle/2438/15850

[22] Benajes, J., García, A., Pastor, J. M., & Monsalve-Serrano, J. (2016). Effects of piston bowl geometry on Reactivity Controlled Compression Ignition heat transfer and combustion losses at different engine loads. Energy, 98, 64–77. https://doi.org/10.1016/j.energy.2016.01.014

[23] Benajes, J., García, A., Monsalve-Serrano, J., Balloul, I., & Pradel, G. (2017). Evaluating the reactivity controlled compression ignition operating range limits in a high-compression ratio medium-duty diesel engine fueled with biodiesel and

ethanol. International Journal of Engine Research, 18(1–2), 66–80. https://doi.org/10.1177/1468087416678500

[24] Benajes, J., García, A., Monsalve-Serrano, J., & Villalta, D. (2018). Exploring the limits of the reactivity controlled compression ignition combustion concept in a light-duty diesel engine and the influence of the direct-injected fuel properties. Energy Conversion and Management, 157(July 2017), 277–287. https://doi.org/10.1016/j.enconman.2017.12.028

[25] Benajes, J., Pastor, J. V, García, A., & Monsalve-Serrano, J. (2015). The potential of RCCI concept to meet EURO VI NOx limitation and ultra-low soot emissions in a heavy-duty engine over the whole engine map. Fuel, 159, 952–961. https://doi.org/10.1016/j.fuel.2015.07.064

[26] Toyir, J., Miloua, R., Elkadri, N. E., Nawdali, M., Toufik, H., Miloua, F., & Saito, M. (2009). Sustainable process for the production of methanol from CO_2 and H_2 using Cu/ZnO-based multicomponent catalyst. Physics Procedia, 2(3), 1075–1079. https://doi.org/10.1016/j.phpro.2009.11.065

[27] Bhardwaj, O. P., Kolbeck, A. F., Kkoerfer, T., & Honkanen, M. (2013). Potential of Hydrogenated Vegetable Oil (HVO) in Future High Efficiency Combustion System. SAE International Journal of Fuels and Lubricants, 6(1), 2013-01–1677. https://doi.org/10.4271/2013-01-1677

[28] Neste Corporation. (2016). Neste Renewable Diesel Handbook. Neste Propietrary Publication, 1–56. https://www.neste.com/sites/default/files/attachments/neste_renewable_diesel_handbook.pdf . Accessed in September, 2019.

[29] Omari, A., Heuser, B., & Pischinger, S. (2017). Potential of oxymethylenether-diesel blends for ultra-low emission engines. Fuel, 209(July), 232–237. https://doi.org/10.1016/j.fuel.2017.07.107

[30] Deutz, S., Bongartz, D., Heuser, B., Kätelhön, A., Schulze Langenhorst, L., Omari, A., Walters, M., Klankermayer, J., Leitner, W., Mitsos, A., Pischinger, S., & Bardow, A. (2018). Cleaner production of cleaner fuels: wind-to-wheel – environmental assessment of CO_2 -based oxymethylene ether as a drop-in fuel. Energy & Environmental Science, 11(2), 331–343. https://doi.org/10.1039/C7EE01657C

[31] Bongartz, D., Burre, J., & Mitsos, A. (2019). Production of Oxymethylene Dimethyl Ethers from Hydrogen and Carbon Dioxide—Part I: Modeling and Analysis for OME 1. Industrial & Engineering Chemistry Research, 58(12), 4881–4889. https://doi.org/10.1021/acs.iecr.8b05576

[32] Burre, J., Bongartz, D., & Mitsos, A. (2019). Production of Oxymethylene Dimethyl Ethers from Hydrogen and Carbon Dioxide—Part II: Modeling and Analysis for OME 3–5. Industrial & Engineering Chemistry Research, 58(14), 5567–5578. https://doi.org/10.1021/acs.iecr.8b05577

[33] Held, M., Tönges, Y., Pélerin, D., Härtl, M., Wachtmeister, G., & Burger, J. (2019). On the energetic efficiency of producing polyoxymethylene dimethyl ethers from CO_2 using electrical energy. Energy & Environmental Science, 12(3), 1019–1034. https://doi.org/10.1039/C8EE02849D

[34] García, A., Gil, A., Monsalve-Serrano, J., & Lago Sari, R. (2020). OMEx-diesel blends as high reactivity fuel for ultra-low NOx and soot emissions in the dual-mode dual-fuel combustion strategy. Fuel, 275(February), 117898. https://doi.org/10.1016/j.fuel.2020.117898

[35] Benajes, J., García, A., Monsalve-Serrano, J., & Villalta, D. (2018). Benefits of E85 versus gasoline as low reactivity fuel for an automotive diesel engine operating in reactivity controlled compression ignition combustion mode. Energy Conversion and Management, 159(December 2017), 85–95. https://doi.org/10.1016/j.enconman.2018.01.015

[36] Benajes, J., García, A., Monsalve-Serrano, J., & Lago Sari, R. (2018). Fuel consumption and engine-out emissions estimations of a light-duty engine running in dual-mode RCCI/CDC with different fuels and driving cycles. Energy, 157, 19–30. https://doi.org/10.1016/j.energy.2018.05.144

[37] Molina, S., García, A., Monsalve-Serrano, J., & Estepa, D. (2018). Miller cycle for improved efficiency, load range and emissions in a heavy-duty engine running under reactivity controlled compression ignition combustion. Applied Thermal Engineering, 136 (December 2017), 161–168. https://doi.org/10.1016/j.applthermaleng.2018.02.106

[38] Benajes, J., García, A., Monsalve-Serrano, J., & Boronat, V. (2017). Gaseous emissions and particle size distribution of dual-mode dual-fuel diesel-gasoline concept from low to full load. Applied Thermal Engineering, 120, 138–149. https://doi.org/10.1016/j.applthermaleng.2017.04.005

[39] Systems, E. M. (2019). Emission Measurement Systems - HORIBA. 1–3. https://www.horiba.com/en_en/products/by-segment/automotive-test-systems/emissions-measurement-systems/ . Accessed in February, 2020.

[40] AVL. (2005). Smoke Value Measurements with the Filter-Paper-Method (Issue June).

[41] Payri, F., Olmeda, P., Martin, J., & Carreño, R. (2014). A New Tool to Perform Global Energy Balances in DI Diesel Engines. SAE International Journal of Engines, 7(1), 2014-01–0665. https://doi.org/10.4271/2014-01-0665

[42] Burger, M., Schmehl, R., Prommersberger, K., Schäfer, O., Koch, R., & Wittig, S. (2003). Droplet evaporation modeling by the distillation curve model: accounting for kerosene fuel and elevated pressures. International Journal of Heat and Mass Transfer, 46(23), 4403–4412. https://doi.org/10.1016/S0017-9310(03)00286-2

[43] Wasewar, K. L., & Sarathi, J. V. (2008). CFD Modelling and Simulation of Jet Mixed Tanks. Engineering Applications of Computational Fluid Mechanics, 2(2), 155–171. https://doi.org/10.1080/19942060.2008.11015218

[44] Pastor, J. V., Garcia-Oliver, J. M., Pastor, J. M., & Vera-Tudela, W. (2015). ONE-DIMENSIONAL DIESEL SPRAY MODELING OF MULTICOMPONENT FUELS. Atomization and Sprays, 25(6), 485–517. https://doi.org/10.1615/AtomizSpr.2014010370

[45] PASTOR, J., JAVIERLOPEZ, J., GARCIA, J., & PASTOR, J. (2008). A 1D model for the description of mixing-controlled inert diesel sprays. Fuel, 87(13–14), 2871–2885. https://doi.org/10.1016/j.fuel.2008.04.017

[46] European Parliament And The Council Of The European Union. (2018). Regulation (EC) No 595/2009 of The European Parliament and of the Council of 18 June 2009 on type-approval of motor vehicles and engines with respect to emissions from heavy duty vehiclec (Euro VI) and amending Regulation (EC) No 715/2007 and Directive 20. 52(68), 48–119. http://data.europa.eu/eli/reg/2009/595/oj

[47] Benajes, J., Garcia, A., Monsalve-Serrano, J., & Sari, R. (2018). Evaluating the Efficiency of a Conventional Diesel Oxidation Catalyst for Dual-Fuel RCCI Diesel-Gasoline Combustion. SAE Technical Papers, 2018-Septe, 1–13. https://doi.org/10.4271/2018-01-1729

[48] Gamma Technologies. (2019). GT-POWER Engine Simulation Software | Gamma Technologies. https://www.gtisoft.com/gt-suite-applications/propulsion-systems/gt-power-engine-simulation-software/ . Accessed in March, 2020.

[49] García, A., Monsalve-Serrano, J., Rückert Roso, V., & Santos Martins, M. E. (2017). Evaluating the emissions and performance of two dual-mode RCCI combustion strategies under the World Harmonized Vehicle Cycle (WHVC). Energy Conversion and Management, 149, 263–274. https://doi.org/10.1016/j.enconman.2017.07.034

[50] García, A., Monsalve-Serrano, J., Villalta, D., & Sari, R. (2019). Octane number influence on combustion and performance parameters in a Dual-Mode Dual-Fuel engine. Fuel, 258(July), 116140. https://doi.org/10.1016/j.fuel.2019.116140

[51] García, A., Monsalve-Serrano, J., Villalta, D., & Lago Sari, R. (2019). Performance of a conventional diesel aftertreatment system used in a medium-duty multi-cylinder dual-mode dual-fuel engine. Energy Conversion and Management, 184(February), 327–337. https://doi.org/10.1016/j.enconman.2019.01.069

[52] Piqueras, P., García, A., Monsalve-Serrano, J., & Ruiz, M. J. (2019). Performance of a diesel oxidation catalyst under diesel-gasoline reactivity controlled compression ignition combustion conditions. Energy Conversion and Management, 196(February), 18–31. https://doi.org/10.1016/j.enconman.2019.05.111

[53] Ogren, R. M. (2015). Development and applications of various optimization algorithms for diesel engine combustion and emissions optimization [Oiwa State University]. https://lib.dr.iastate.edu/etd/14965

[54] Benajes, J., García, A., Monsalve-Serrano, J., & Martínez-Boggio, S. (2020). Potential of using OMEx as substitute of diesel in the dual-fuel combustion mode to reduce the global CO_2 emissions. Transportation Engineering, 1(January), 100001. https://doi.org/10.1016/j.treng.2020.01.001

[55] Data sheets - Volvo Trucks Saudi Arabia. (n.d.). https://www.volvotrucks.com/en-sa/trucks/volvo-fe/specifications/data-sheets.html. Accessed in June, 2019.

Abbreviations

AF: Air-to-fuel ratio

ATDC: After Top Dead Center

BMEP: Brake Mean Effective Pressure

BSCO: Brake Specific CO emissions

BSFC: Brake Specific Fuel Consumption

BSHC: Brake Specific Hydrocarbons emissions

BSNOx: Brake Specific NOx emissions

BSSoot: Brake Specific Soot emossions

BTDC: Before Top Dead Center

CAD: Crank Angle Degree

CA10: Crank angle for 10% of burned fuel mass

CA50: Crank angle for 50% of burned fuel mass

CA90: Crank angle for 90% of burned fuel mass

CI: Compression Ignition

CO: Carbon Monoxide

CO_2: Carbon Dioxide

COV: Coefficient of Variation

DI: Direct Injection

DMDF: Dual Mode Dual Fuel

DOC: Diesel Oxidation Catalyst

EGR: Exhaust Gas Recirculation

FSN: Filter Smoke Number

GF: Gasoline Fraction

HC: Hydrocarbons

HCCI: Homogeneous Charge Compression Ignition

HFI: High Flow Injector

HRR: Heat Release Rate

HRF: High Reactivity Fuel

HVO: Hydrogenated/hydro treated vegetable oil

ICE: Internal Combustion Engine

IMEP: Indicated Mean Effective Pressure

LFI: Low Flow Injector

LHV: Lower Heating Value

LRF: Low Reactivity Fuel

LTC: Low Temperature Combustion

MCE: Multi Cylinder Engine

NOx: Nitrogen Oxides

OMEx: Oxymethylene dimethyl ethers mixture

PER: Premixed Energy Ratio

PFI: Port Fuel Injection

PPC: Partially Premixed Combustion

RoHR: Rate of Heat Release

RCCI: Reactivity Controlled Compression Ignition

SI: Spark Ignition

TDC: Top Dead Center

Symbols

P: Pressure

T: Temperature

m: mass

t: time

ρ: Density

μ: Viscosity

Subscripts

a: referred to air

D: referred to diesel

eq: referred to equivalent conditions

evap: referred to the evaporation process

f: referred to fuel

referred to gasoline

mix: referred to the mixing process

OMEx: referred to OMEx

st: referred to stoichiometric conditions

vap: referred to vapor conditions

t: target value